The Journal of Experimental Biology 212, 1003-1010
Published by The Company of Biologists 2009
doi:10.1242/jeb.025957

Morphological and functional classification of ion-absorbing mitochondria-rich cells in the gills of Mozambique tilapia

Mayu Inokuchi*[,1], Junya Hiroi[2], Soichi Watanabe[1], Pung-Pung Hwang[3] and Toyoji Kaneko[1]

[1]Department of Aquatic Bioscience, Graduate School of Agricultural and Life Sciences, The University of Tokyo, Bunkyo, Tokyo 113-8657, Japan, [2]Department of Anatomy, St Marianna University School of Medicine, Kawasaki, Kanagawa 216-8511, Japan and [3]Institute of Cellular and Organismic Biology, Academia Sinica, Nankang, Taipei 11529, Taiwan

*Author for correspondence (e-mail: niida@marine.fs.a.u-tokyo.ac.jp)

Accepted 19 January 2009

SUMMARY

To clarify ion-absorbing functions and molecular mechanisms of mitochondria-rich (MR) cells, Mozambique tilapia (*Oreochromis mossambicus*) were acclimated to artificial freshwaters with normal or lowered Na^+ and/or Cl^- concentration: (1) normal Na^+/normal Cl^- (control); (2) normal Na^+/low Cl^-; (3) low Na^+/normal Cl^-; and (4) low Na^+/low Cl^-. Scanning electron microscopy (SEM) revealed that concave and convex apical surfaces of MR cells predominantly developed in low Na^+ and low Cl^- waters, respectively, whereas small apical pits predominated in control conditions. Expression of Na^+/H^+ exchanger-3 (NHE3) mRNA in the gills was increased in low Na^+ waters (low Na^+/normal Cl^- and low Na^+/low Cl^-), whereas that of Na^+/Cl^- cotransporter (NCC) expression was upregulated in low Cl^-, but not in low Na^+/low Cl^-. Immunofluorescence staining showed that enlarged NHE3-immunoreactive apical regions were concave or flat in low Na^+ waters, whereas NCC-immunoreactive regions were enlarged convexly in low Cl^- waters. Using SEM immunocytochemistry the distribution of NHE3/NCC was compared with SEM images obtained simultaneously, it was further demonstrated that NHE3 and NCC were confined to concave and convex apical surfaces, respectively. These results indicated that small apical pits developed into concave apical surfaces to facilitate Na^+ uptake through NHE3, and into convex apical surfaces to enhance Na^+/Cl^- uptake through NCC. Our findings integrated morphological and functional classifications of ion-absorbing MR cells in Mozambique tilapia.

Key words: Na^+/H^+ exchanger-3, Na^+/Cl^- cotransporter, mitochondria-rich cell, Mozambique tilapia, gill morphology.

INTRODUCTION

Euryhaline teleosts inhabiting both freshwater and seawater maintain their plasma osmolalities within narrow physiological ranges, equivalent to about one-third seawater osmolality. The gills, kidney and intestine are important osmoregulatory organs in fish, creating ionic and osmotic gradients between the body fluid and external environments (Marshall and Grosell, 2006). In particular, mitochondria-rich (MR) cells, also referred to as chloride cells, in the gills are important in maintaining ionic balance in fish (Kaneko et al., 2008). It is well established that gill MR cells are responsible for salt secretion in seawater-adapted fish, and the molecular mechanism of salt secretion has been well documented (Evans et al., 2005). By contrast, MR cells in freshwater-adapted teleosts are responsible for ion uptake, but the mechanisms involved are still poorly understood (Marshall, 2002; Hirose et al., 2003; Perry et al., 2003; Evans et al., 2005; Hwang and Lee, 2007).

In freshwater-adapted fish, three ion-transport proteins have been proposed as the apical pathways for sodium uptake in MR cells. Sodium–hydrogen exchanger-3 (NHE3) in the apical membrane of gill MR cells has been advocated as one possible pathway for Na^+ uptake and H^+ secretion in Japanese dace *Tribolodon hakonensis* (Hirata et al., 2003), zebrafish *Danio rerio* (Yan et al., 2007), tilapia *Oreochromis mossambicus* (Watanabe et al., 2008) and Atlantic stingray *Dasyatis sabina* (Choe et al., 2005). Meanwhile, a model consisting of vacuolar-type H^+-ATPase (V-ATPase) electrically coupled to a conductive Na^+ channel has been proposed as a Na^+-uptake mechanism: Na^+ is absorbed *via* apically located Na^+ channels in exchange for H^+ secreted by V-ATPase (Fenwick et al., 1999; Katoh et al., 2003; Lin et al., 2006; Esaki et al., 2007). Most recently, it has been demonstrated that Na^+/Cl^- cotransporter (NCC) is located in the apical membrane of MR cells in the embryonic skin of freshwater-adapted tilapia (Hiroi et al., 2008). NCC is presumably responsible for Na^+ and Cl^- uptake from hypotonic water. Our previous study showed that both apical NHE3 and NCC, rather than V-ATPase, are importantly involved in ion uptake in gill MR cells of tilapia acclimated to hypotonic environments (Inokuchi et al., 2008).

Morphological changes in MR cells in response to environmental salinity have been observed in several teleost species. On the basis of transmission electron microscopic observations, MR cells in the gills were classified into α and β types in several teleosts (Pisam et al., 1987; Pisam et al., 1990; Pisam et al., 1995). During seawater acclimation, α cells, located at the base of the lamellae, were transformed into seawater-type MR cells, whereas β cells, in the interlamellar region, degenerated and disappeared. By contrast, scanning electron microscopic (SEM) observations showed that the apical structure of MR cells varied greatly among teleost species (Perry et al., 1992). Although the apical membrane of MR cells in seawater typically forms a pit, in freshwater it generally appears as a flat or slightly projecting disk. In tilapia and other species, however, the pit structure of the apical membrane is also observed in freshwater (Perry, 1997; Uchida et al., 2000; Inokuchi et al., 2008). In freshwater-acclimated tilapia, three subtypes of MR cells with different apical-surface structures were identified in the gills: wavy-convex, shallow-basin and deep-hole MR cells (Lee et al., 1996). Wavy-convex and shallow-basin MR cells are considered to absorb

Cl^- and Ca^{2+}, respectively, but the subtype responsible for Na^+ uptake has not been identified (Chang et al., 2001; Chang et al., 2003). Wavy-convex MR cells are characterized by a wide apical opening and a rough surface appearance. By using confocal laser scanning and differential interference contrast microscopy, it was observed that the ion-absorbing MR cells, in which NCC was localized in the apical membrane, possessed a wide apical opening and a rough apical surface (Hiroi et al., 2005; Hiroi et al., 2008). Therefore, those ion-absorbing cells are likely to be identical to the wavy-convex MR cells. However, the evident relationship between variable morphology of apical surface and localization of ion-transport proteins is still unclear.

In the present study, we aimed to clarify ion-absorbing functions and molecular mechanisms of MR cells with special reference to alterations of their apical structure in Mozambique tilapia. In fish acclimated to artificial freshwaters with lowered Na^+ and/or Cl^- concentration, we examined the apical morphology of MR cells, expression of NHE3 mRNA and NCC mRNA in the gills, and their immunolocalization in MR cells. To further clarify the relationship between the apical morphology and occurrence of NHE3 and NCC in MR cells, we attempted the simultaneous observation of SEM images and the distribution patterns of NHE3 and NCC by means of SEM immunocytochemistry. Our findings indicate that MR cells developed concave and convex apical surfaces in low Na^+ and Cl^- conditions, respectively. Our findings also revealed differential distribution of NHE3 and NCC in concave and convex apical surfaces, respectively.

MATERIALS AND METHODS

Fish

Mozambique tilapia (*Oreochromis mossambicus* Peters) were maintained in tanks supplied with recirculating freshwater, and water temperature was maintained at 25°C. Fish were fed on commercial tilapia pellets 'Tilapia 41M' (Nishinihon Kumiai Shiryo, Hyogo, Japan) once a day. Four groups of freshwater-acclimated tilapia, mass 58–147 g, were exposed to artificial freshwaters with different Na^+ and Cl^- concentrations: (1) normal Na^+/normal Cl^- (Control); (2) normal Na^+/low Cl^- (LowCl); (3) low Na^+/normal Cl^- (LowNa); and (4) low Na^+/low Cl^- (LowNa/LowCl). Fish were kept in 100 l plastic tanks containing the respective media for 1 week at 25°C without feeding. Each group consisted of eight individuals. Half the water was changed every other day to guarantee optimal water quality. Artificial freshwaters were prepared by dissolving appropriate amounts of NaCl, Na_2SO_4, $MgSO_4$, K_2HPO_4, KH_2PO_4, $CaCl_2$ and $CaSO_4$ in deionized water, according to the method described in previous studies (Chang et al., 2001; Chang et al., 2002; Chang et al., 2003; Lin and Hwang, 2004). The pH of the media was between 6.65 and 6.75. The ion composition and concentration of Control water mimicked local freshwater, the nominated concentrations of Na^+ and Cl^- being 1.0 mmol l^{-1} each, while freshwater with low Na^+ and low Cl^- did not contain Na^+ and Cl^-, respectively. Actual ion concentrations in the four media were determined with an ion analyzer (IA-200, TOA-DKK, Tokyo, Japan). Table 1 shows ion concentrations of the four media on the first and last days of the experiment.

Plasma osmolality and ion concentrations

Plasma osmolality and Na^+ and Cl^- concentrations were measured in tilapia exposed to the four experimental media. After fish were anesthetized with 0.1% 2-phenoxyethanol, blood was collected from the caudal vessels with a heparinized syringe and needle. The blood plasma was separated by centrifugation and stored at –20°C. Later, plasma osmolality was measured with a vapor pressure osmometer (Wescor 5520, Logan, UT, USA), and plasma Na^+ and Cl^- concentrations were measured using the ion analyzer (IA-200) and a digital chloridometer (Labconco, Kansas, MO, USA), respectively.

Gill sampling

After blood sampling, gill filaments were removed from the first gill arches and frozen in liquid nitrogen for total RNA extraction. For SEM, the second gills were dissected out, fixed in 2% paraformaldehyde (PFA)–2% glutaraldehyde (GA) in 0.1 mol l^{-1} phosphate buffer (PB, pH 7.4) for 24 h at 4°C, and stored in 70% ethanol. For whole-mount immunocytochemistry and SEM immunocytochemistry, the second gills of the other side were fixed in 4% PFA in PB for 24 h at 4°C, and stored in 70% ethanol.

Scanning electron microscopic observation

Gill filaments were removed from the gills fixed for SEM, dehydrated in ethanol, immersed in *t*-butylalcohol, and dried in a freeze-drying device (VFD-21, Vacuum Device, Ibaragi, Japan). Dried samples were mounted on specimen stubs, coated with platinum–palladium in an ion sputter (Hitachi E-1030, Tokyo, Japan), and examined with a Hitachi S-4000 SEM. For the quantitative analysis, the density of MR cells was determined with Image-Pro Plus (Media Cybernetics, Silver Spring, MD, USA). One field, corresponding to 6075 μm^2, at the flat region of the afferent-vascular side of a gill filament was randomly selected from each fish, and the number of MR cells in the field was counted. Data were obtained from eight individuals in each experimental group, and expressed as the cell number per millimeter squared.

Real-time quantitative-PCR

Expression levels of NHE3 and NCC mRNAs were determined by real-time quantitative-PCR with a LightCycler ST300 (Roche Diagnostic, Penzberg, Germany) and LightCycler FastStart DNA Master SYBR Green I (Roche Diagnostic). Total RNA was extracted with RNA extraction solution (Isogen, Nippon Gene, Toyama, Japan) from the gill filaments. Total RNA was treated with DNase (Invitrogen, Carlsbad, CA, USA), and then reverse-transcribed using a Superscript First-Strand Synthesis System for RT-PCR (Invitrogen). For the detection of NHE3 (GenBank accession no. AB326212) and NCC (EU518934) mRNAs, specific primers were designed as follows: NHE3, ATG GCG TGT GGA GGC TTG (forward) and CCT GTC CCA GTT TCT GTT TGT G (reverse); and NCC, CCG AAA GGC ACC CTA ATG G (forward) and CTA

Table 1. Ion concentrations (mmol l^{-1}) of the four experimental media

Medium	$[Na^+]$	$[Cl^-]$	$[K^+]$	$[Ca^{2+}]$	$[Mg^{2+}]$
Control	0.95/0.99	1.00/1.03	0.21/0.23	0.62/0.71	0.26/0.30
LowCl	0.94/0.97	0.02/<0.01	0.20/0.22	0.65/0.69	0.28/0.29
LowNa	<0.01/0.01	0.97/1.01	0.20/0.23	0.65/0.70	0.27/0.29
LowNa/LowCl	<0.01/0.01	0.01/0.01	0.22/0.23	0.69/0.70	0.28/0.29

Concentrations are in mmol l^{-1}; values of the first/last day.

CAC TTG CAC CAG AAG TGA CAA (reverse). The copy number of the transcripts was calculated with reference to the parallel amplifications of known concentrations of the respective cloned PCR fragments. The data were normalized with the expression levels of 18S rRNA measured in parallel. Expression of 18S rRNA was quantified with a primer pair, CGA TGC TCT TAG CTG AGT GT (forward) and ACG ACG GTA TCT GAT CGT CT (reverse).

Antibodies

For immunocytochemical detection of Na^+/K^+-ATPase-immunoreactive MR cells, we used a rabbit polyclonal antiserum raised against a synthetic peptide corresponding to part of the highly conserved region of the Na^+/K^+-ATPase α-subunit (NAK121) (Uchida et al., 2000). The specificity of the antibody was determined by Uchida et al. (Uchida et al., 2000). To detect NHE3, a polyclonal antibody was raised in a rabbit against a synthetic peptide corresponding to a C-terminal region of tilapia NHE3 (Watanabe et al., 2008). The antibody to detect NCC was a mouse monoclonal antibody directed against 310 amino acids at the C terminus of human colonic NKCC1 (T4; developed by Christian Lytle and Bliss Forbush III, and obtained from the Developmental Studies Hybridoma Bank, IA, USA). The T4 antibody has been shown to react with NCC in the apical region of MR cells of tilapia acclimated to hypotonic water (Hiroi et al., 2005; Hwang and Lee, 2007; Hiroi et al., 2008; Inokuchi et al., 2008), thus being referred to as anti-NCC in the present study.

Triple-color whole-mount immunofluorescence staining

Gill filaments were removed from the gills fixed in 4% PFA in PB, washed in 0.01 mol l^{-1} phosphate-buffered saline containing 0.2% Triton X-100 (PBST) for 1 h, and incubated with a mixture of anti-NHE3 and anti-NCC for 2 days at room temperature. Anti-NHE3 and anti-NCC were diluted 1:250 and 1:500, respectively, with PBST containing 10% normal goat serum, 0.1% bovine serum albumin, 0.02% keyhole limpet hemocyanin and 0.01% sodium azide (NB-PBS). The samples were then incubated overnight at room temperature with a mixture of goat anti-rabbit IgG labeled with Alexa Fluor 488 and goat anti-mouse IgG labeled with Alexa Fluor 405 (Molecular Probes, OR, USA), both diluted 1:500 with NB-PBS. The filaments were washed in PBST, and subjected to post-staining fixation with 4% PFA in PB for 1 h. After washing in PBST, samples were incubated with Alexa Fluor 546-labeled anti-Na^+/K^+-ATPase (Katoh et al., 2003) diluted 1:500 with NB-PBS for 3 days at room temperature. The samples were observed with a confocal laser scanning microscope (C1, Nikon, Tokyo, Japan). The wavelengths of excitation and recorded emission for each Alexa dye were as follows: Alexa Fluor 546, 543 nm and 605/75 nm; Alexa Fluor 488, 488 nm and 515/30 nm; and Alexa Fluor 405, 405 nm and 450/35 nm.

Horizontal-section images of MR cells were obtained by viewing the flat region of the afferent-vascular side of gill filaments with the confocal laser scanning microscope. Serial confocal images were overlaid to produce a panfocal image. To obtain cross-section images of MR cells, those located at the afferent edge were observed. By adjusting the focal plane, optical sections cut through the apical membrane of MR cells can be readily observed.

Scanning electron microscopic immunocytochemistry

After a rinse with PBST for 1 h, the gill filaments fixed in 4% PFA in PB were incubated either with anti-NHE3 (diluted 1:250 with NB-PBS) or with anti-NCC (1:500) overnight at room temperature. The samples were rinsed with PBST and then incubated overnight at room temperature with secondary antibody conjugated with 10 nm gold particles (British Biocell International, Cardiff, UK). The secondary antibodies for anti-NHE3 and anti-NCC were goat anti-rabbit IgG and goat anti-mouse IgG, respectively, both diluted 1:50 with NB-PBS. After the gill filaments were washed in PBST, gold particles were silver-enhanced for 10–15 min at room temperature with Silver Enhancing Kit (British Biocell International). The reaction was stopped by rinsing the sample with distilled water. After post-staining fixation with 2% PFA–2% GA in PB for 1 h, the gill filaments were dehydrated in ethanol, immersed in *t*-butylalcohol, and dried in the freeze-drying device (VFD-21). Dried samples were mounted on specimen stubs, coated with gold in an ion sputter (IB3, Eiko, Tokyo, Japan), and examined with the Hitachi S-4000 SEM equipped with an energy-dispersive X-ray microanalyzer (EMAX-5770, Horiba, Kyoto, Japan) and a Super Xerophy X-ray detector (Horiba). The elemental profile of Ag was examined by detecting the X-ray characteristic of Ag at 2.986 keV (Lα1). The SEM image and the distribution pattern of Ag at the corresponding area were obtained to correlate the apical structure of MR cells with the occurrence of the ion-transport proteins. The specificity of immunoreactions was confirmed by incubating the tissues in preimmune rabbit serum and mouse IgG in place of the specific antibodies as negative controls for NHE3 and NCC, respectively.

Statistics

Data are presented as means ± standard error of the mean. The significance of differences at $P<0.05$ was examined by one-way analysis of variance (ANOVA), followed by Fisher's PLSD (StatView, SAS Institute, Cary, NC, USA).

RESULTS

Plasma osmolality and ion concentrations

No mortality was observed during the experiment period of 1 week. Mean plasma osmolalities of tilapia in the Control, LowCl, LowNa and LowNa/LowCl groups ranged between 296 and 320 mosmol kg^{-1} (Table 2). Plasma osmolality was significantly lower in the LowCl, LowNa and LowNa/LowCl groups than in the Control.

Although plasma Na^+ and Cl^- concentrations stayed within narrow ranges in all experimental groups, plasma Na^+ and Cl^- concentrations tended to be lower at low levels of environmental Na^+ and Cl^-, respectively (Table 2). Plasma Na^+ concentration was significantly lower in the LowNa and LowNa/LowCl than in Control groups. Plasma Cl^- concentration was significantly higher in the Control than in any other group.

Table 2. Plasma osmolality and Na^+ and Cl^- concentrations of tilapia

Medium	Control	LowCl	LowNa	LowNa/LowCl
Plasma osmolality (mosmol kg^{-1})	320.4±1.5	309.4±3.0*	307.8±1.8*	296.5±2.8*
Plasma Na^+ concentration (mmol l^{-1})	159.2±1.7	159.6±1.2	151.3±1.5*	150.3±1.8*
Plasma Cl^- concentration (mmol l^{-1})	141.9±1.5	132.8±1.1*	135.4±1.4*	130.0±1.8*

Values are expressed as the mean ± s.e.m. (N=8).
*$P<0.05$ compared with the Control group.

Scanning electron microscopic observation

MR cells in the gills were in contact with the external environment through their apical membrane, which was located at the boundary of pavement cells with ridge structures on their surface. The external structure of the apical membrane of MR cells varied greatly among the four experimental groups (Fig. 1). The apical structures of MR cells found in the gill filaments were classified into the following three types: (1) a small apical pit; (2) a concave apical surface; and (3) a convex apical surface. Small apical pits were narrow and deep, so that little or no internal structure could be observed. Concave apical surfaces were slightly dented, or sometimes flat, with a mesh-like structure on their surface. Convex apical surfaces were equipped with microvilli, presenting a convex rough surface. Both concave and convex apical surfaces varied greatly in size (Fig. 1). Concave and convex apical surfaces predominantly developed in the gills of tilapia acclimated to LowNa and LowCl, respectively, whereas small apical pits predominated in Control fish (Fig. 1A–C). Both concave and convex surfaces were frequently observed in the LowNa/LowCl group (Fig. 1D). However, convex apical surfaces were more enlarged in LowCl than in LowNa/LowCl groups (Fig. 1B,D). The quantitative analysis showed that the frequency of the three types of MR cells differed greatly among the experimental groups (Fig. 2). The density of small apical pits was highest in the Control and lowest in LowNa/LowCl. The concave apical surfaces were more frequently observed in fish in media with low Na^+ (LowNa and LowNa/LowCl) than in those with normal Na^+ (Control and LowCl). However, convex apical surfaces were fewer in the Control than in any other group. Convex apical surfaces were more numerous in the LowCl than in the LowNa, whereas there was no significant difference between the LowCl and LowNa/LowCl and between the LowNa and LowNa/LowCl groups. Some apical surfaces (less than 6%) of MR cells were unclassified, since their apical structures did not fall typically into the three categories or showed some intermediate characteristics.

Real-time quantitative-PCR

The expression levels of NHE3 mRNA in the gills were significantly increased in the LowNa and LowNa/LowCl groups than in the Control and LowCl groups (Fig. 3A). The expression of NHE3 in LowNa and LowNa/LowCl was about threefold higher than that in Control and LowCl groups. However, the expression of NCC mRNA was significantly increased only in LowCl, while there was no significant difference among Control, LowNa and LowNa/LowCl groups (Fig. 3B). The expression level of NCC in the LowCl group were about fourfold higher than in Control and LowNa/LowCl, and eightfold higher than in LowNa groups.

Whole-mount immunocytochemistry for NHE3 and NCC

The immunoreaction for NHE3 and NCC was observed within Na^+/K^+-ATPase-immunoreactive MR cells, but not detected in the other cell types in the gill epithelia (Fig. 4). NHE3 and NCC were localized in the apical region of MR cells, but they were never colocalized in the same cells. Based on distribution patterns of NHE3 and NCC immunoreactivity, most MR cells in the four experimental groups could be classified into two types; that is, cells with apical NHE3 and those with apical NCC; however, a few MR cells were not immunoreactive to either NHE3 or NCC. The shape and size of NHE3- and NCC-immunoreactive apical regions varied greatly among the four experimental groups (Fig. 4). NHE3-immunoreactive apical regions were more enlarged in the LowNa and LowNa/LowCl fish than in the Control and LowCl groups (Fig. 4B,F,J,N). By contrast, NCC-immunoreactive regions were much larger in the LowCl and LowNa/LowCl fish than in Control and LowNa (Fig. 4C,G,K,O).

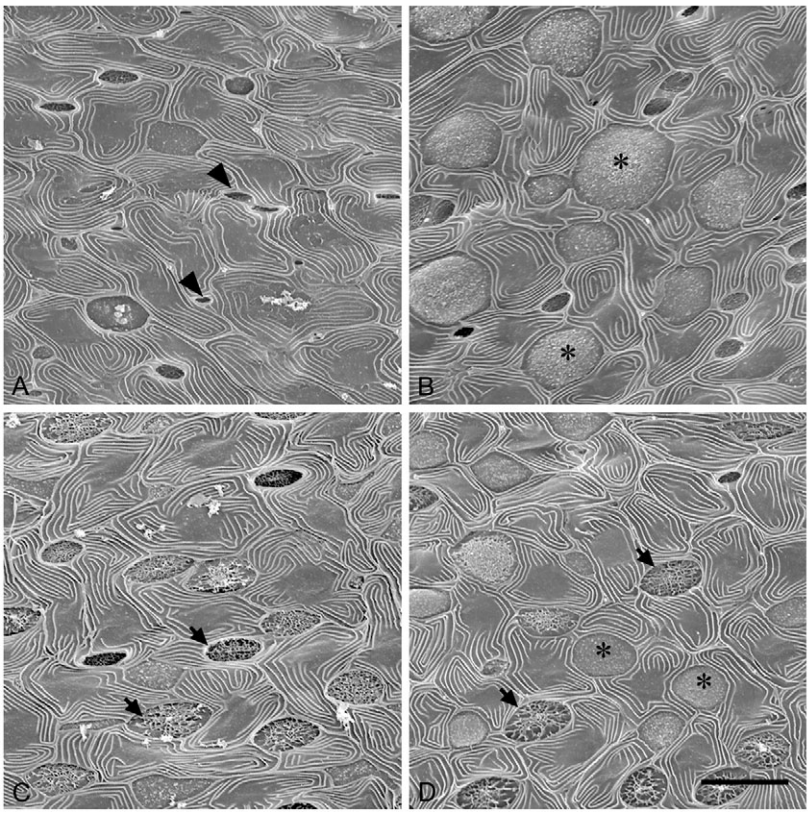

Fig. 1. Scanning electron micrographs of gill filaments of tilapia acclimated to artificial freshwaters with different Na^+ and Cl^- concentrations: normal Na^+/normal Cl^- (Control; A); normal Na^+/low Cl^- (LowCl; B); low Na^+/normal Cl^- (LowNa; C); and low Na^+/low Cl^- (LowNa/LowCl; D). The apical structures of mitochondria-rich cells are classified into the following three types: a small apical pit (arrowhead); a concave apical surface (arrow); and a convex apical surface (asterisk). Small apical pits are narrow and deep, so that little or no internal structure can be observed. Concave apical surfaces are slightly dented, or sometimes flat, with a mesh-like structure on their surface. Convex apical surfaces are equipped with microvilli. Small apical pits predominate in Control fish (A). Concave and convex apical surfaces predominantly develop in LowNa and LowCl fish, respectively (B,C). Both concave and convex surfaces are frequently observed in LowNa/LowCl fish (D). Scale bar, 10 μm.

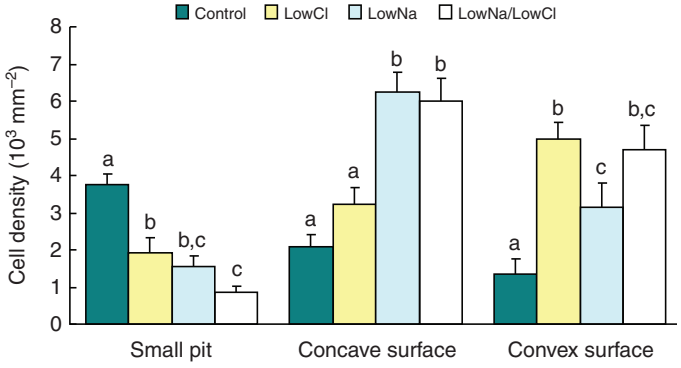

Fig. 2. Densities of different apical types of mitochondria-rich cells (small apical pit, concave apical surface and convex apical surface) in the gills of tilapia acclimated to artificial freshwaters with different Na^+ and Cl^- concentrations: normal Na^+/normal Cl^- (Control); normal Na^+/low Cl^- (LowCl); low Na^+/normal Cl^- (LowNa); and low Na^+/low Cl^- (LowNa/LowCl). Data are expressed as the mean ± s.e.m. (N=8). Different letters indicate significant differences at P<0.05.

Cross-sectional images of MR cells further revealed the difference in the shape of NHE3- and NCC-immunoreactive apical regions (Fig. 5). In Control, small areas of NHE3 and NCC staining often had a cup-like appearance: doughnut-shaped in horizontal sections and U-shaped in the cross-section (Fig. 5A,C,E,G). In MR cells with large apical surface typically seen in the LowCl, LowNa and LowNa/LowCl groups, NHE3-immunoreactive regions appeared to be concave or flat (Fig. 5B,F), whereas NCC-immunoreactive regions had a convex appearance (Fig. 5D,H).

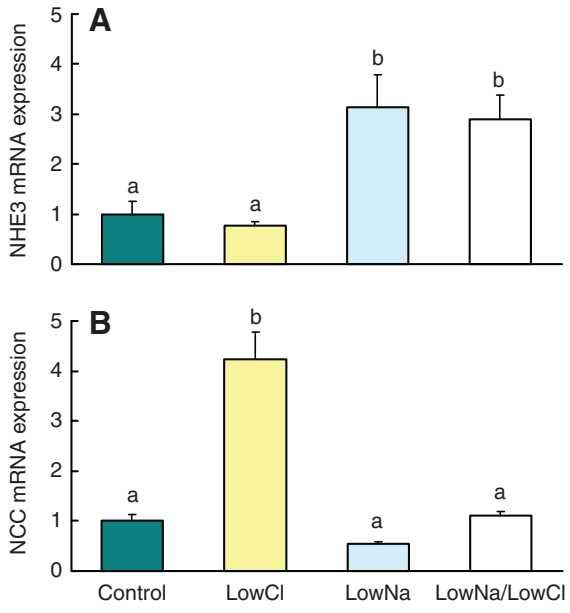

Fig. 3. Relative mRNA expression levels of Na^+/H^+ exchanger-3 (NHE3; A) and Na^+/Cl^- cotransporter (NCC; B) in the gills of tilapia acclimated to artificial freshwaters with different Na^+ and Cl^- concentrations: normal Na^+/normal Cl^- (Control); normal Na^+/low Cl^- (LowCl); low Na^+/normal Cl^- (LowNa); and low Na^+/low Cl^- (LowNa/LowCl). The data are normalized to the expression levels of 18S rRNA. Data are expressed as the mean ± s.e.m. (N=8). Different letters indicate significant differences at P<0.05.

Scanning electron microscopic immunocytochemistry for NHE3 and NCC

To confirm the relationship between the localization of NHE3 and NCC and the structure of the apical membrane of MR cells, the gill filaments of fish acclimated to LowNa/LowCl and LowCl were examined by SEM immunocytochemistry (Fig. 6). In this technique, NHE3/NCC was indirectly labeled with Ag, and X-ray signals specific for Ag were localized by X-ray microanalysis (Fig. 6B,E). Therefore, the immunoreactive site of NHE3 or NCC appeared to be lightly dusted with Ag precipitate (Fig. 6A,D). The distribution patterns of Ag were compared in SEM images obtained simultaneously. The localization of NHE3 was confined to concave apical surfaces of MR cells (Fig. 6A–C). Conversely, NCC was detected only in convex apical surfaces (Fig. 6D–F). These signals disappeared in tissues incubated in preimmune rabbit serum or mouse IgG in place of the specific antibody.

DISCUSSION

In the present study, in order to examine the morphological alteration and the molecular mechanisms of ion uptake in gill MR cells, tilapia were acclimated to artificial freshwaters with different Na^+ and Cl^- concentrations. Plasma osmolality and Na^+ and Cl^- concentrations in fish subjected to the four experimental ion conditions were maintained within physiologically normal ranges (Lee et al., 2000; Uchida et al., 2000), indicating their successful acclimation to those conditions. Within the narrow physiological ranges, however, plasma osmolality and ion levels tended to be lower at lower environmental Na^+ and Cl^- concentrations. When ambient Na^+ and Cl^- levels are extremely low, fish face severe diffusional Na^+ and Cl^- loss and difficulty in absorbing deficient ions. Therefore, MR cells of fish in low Na^+ and Cl^- conditions are expected to enhance ion-absorbing activities. This is in agreement with previous findings that Na^+/K^+-ATPase activity of gill MR cells was significantly higher in tilapia acclimated to deionized freshwater than in those acclimated to normal freshwater (Tang et al., 2008; Inokuchi et al., 2008).

We investigated morphological changes in the structure of the apical membrane of MR cells in the four experimental groups by SEM, and identified three subtypes of apical structures: a small apical pit, a concave apical surface, and a convex apical surface. Small apical pits predominated in the Control group, in which the ambient Na^+ and Cl^- concentrations mimicked those of freshwater. By contrast, convex apical surfaces were prominent in the LowCl group, suggesting that convex apical surfaces are involved in Cl^- uptake. The convex apical surface is considered to be identical to the wavy-convex structure, previously reported in tilapia (Lee et al., 1996; Chang et al., 2001; Chang et al., 2003; Lin and Hwang, 2004) and goldfish (Chang et al., 2002). The apical size and relative density of wavy-convex MR cells were found to increase in low Cl^- conditions and to be positively correlated with Cl^- influx (Chang et al., 2003). Since MR cells are in contact with ambient water *via* their apical surface, the appearance of wavy-convex MR cells with larger apical surface was considered to enhance Cl^- uptake (Chang et al., 2003; Lin and Hwang, 2004).

Meanwhile, a subtype responsible for Na^+ uptake has not yet been identified: it has been considered that pavement cells may be the site for Na^+ uptake rather than MR cells (Goss et al., 1995; Perry, 2003; Laurent et al., 2006). In tilapia, it has also been suggested that pavement cells are responsible for Na^+ uptake (Chang et al., 2003). In the present study, however, concave apical surfaces were greatly enlarged and increased in number in tilapia acclimated to low Na^+. This result suggests that the concave apical surface plays

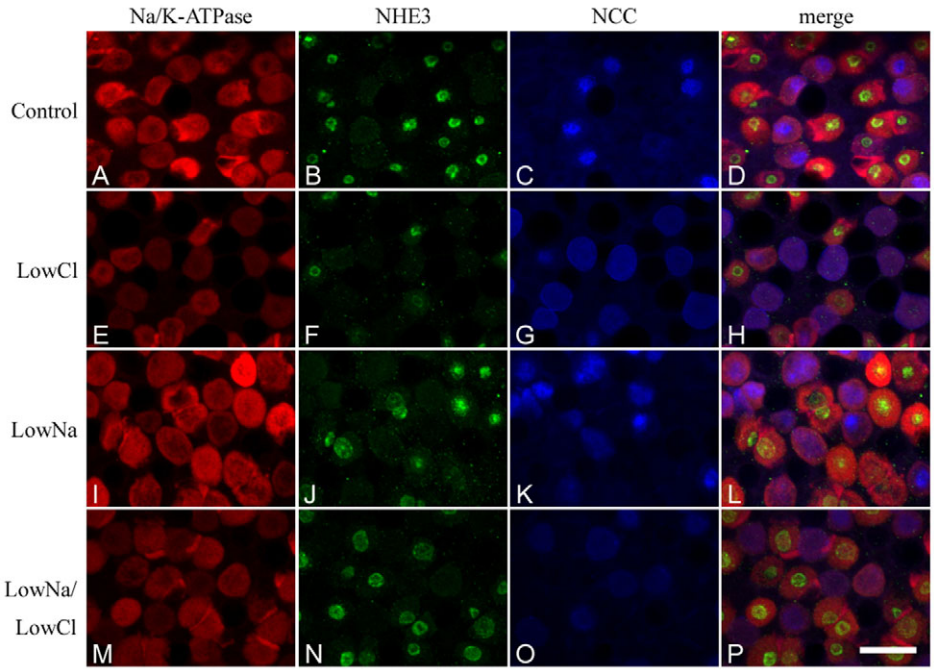

Fig. 4. Triple immunofluorescence staining with anti-Na^+/K^+-ATPase (A,E,I,M, red), anti-NHE3 (B,F,J,N, green) and anti-NCC (C,G,K,O, blue) in gill filaments of tilapia acclimated to artificial freshwaters with different Na^+ and Cl^- concentrations: normal Na^+/normal Cl^- (Control; A–D); normal Na^+/low Cl^- (LowCl; E–H); low Na^+/normal Cl^- (LowNa; I–L); and low Na^+/low Cl^- (LowNa/LowCl; M–P). D,H,L,P, Merged images. Scale bar, 20 μm.

a crucial role in Na^+ uptake. Furthermore, both concave and convex apical surfaces were frequently observed in the LowNa/LowCl group, confirming that concave and convex apical surfaces were responsible for Na^+ and Cl^- uptake. MR cells with large apical surfaces, whose structures were similar to the concave and convex apical surfaces, were also reported in scaleless carp *Gymnocypris przewalskii* (Matey et al., 2008). In killifish *Fundulus heteroclitus*, a branchial epithelial cell type named the 'cuboidal cell' was proposed as the site of Na^+ uptake in the gills. The apical surfaces of these cells were triangular, square or rounded, and were either smooth or villous in surface relief (Laurent et al., 2006). In terms of Na^+-absorbing nature, concave-apical MR cells might be identical to cuboidal cells, although further investigation is required to address this issue.

Our previous study showed that NHE3 and NCC were critical for ion uptake in gill MR cells of tilapia acclimated to hypotonic water (Hiroi et al., 2008; Inokuchi et al., 2008). In this study, to clarify the molecular mechanisms for Na^+ and Cl^- uptake, we compared the expressions of NHE3 and NCC in the gills of tilapia acclimated to artificial freshwaters with different Na^+ and Cl^- concentrations. Expression levels of NHE3 mRNA in the gills were increased in the LowNa and LowNa/LowCl groups. This result indicates that NHE3 is involved in Na^+ uptake under low Na^+ conditions. Similarly, in zebrafish gills, the expression of NHE3b was upregulated in a low Na^+ environment (Yan et al., 2007). Furthermore, it was demonstrated that EIPA, a selective inhibitor of NHE, blocked Na^+ accumulation in MR cells of the zebrafish embryonic skin, supporting the involvement of NHE in Na^+ absorption (Esaki et al., 2007). Meanwhile, NCC was shown to be responsible for Na^+ and Cl^- uptake in MR cells (Hiroi et al., 2008). Expression of NCC mRNA was upregulated in our LowCl fish, suggesting that NCC plays a critical role in Cl^- uptake. However, NCC mRNA expression was not induced in the LowNa/LowCl group. The higher expression of NCC in the LowCl than in LowNa/LowCl group is consistent with our SEM observation that the area of convex apical surfaces is larger in the LowCl group than in LowNa/LowCl group. It may be possible that another ion transporter is involved in Cl^- uptake when both Na^+ and Cl^- concentrations are extremely low. It has been considered that Cl^- uptake in the gills is mediated by a Cl^-/HCO_3^- anion exchanger (Evans et al., 2005). Immunocytochemical studies with a polyclonal antibody against rainbow trout erythrocyte Cl^-/HCO_3^- anion exchanger-1 have shown that the Cl^-/HCO_3^- anion exchanger is localized in the apical membrane of tilapia and coho salmon MR cells (Wilson et al., 2000; Wilson et al., 2002). However, only a few studies have examined this putative Cl^- uptake pathway, and there is still no convincing evidence that Cl^-/HCO_3^- anion exchanger functions as a molecule responsible for apical Cl^- uptake in MR cells.

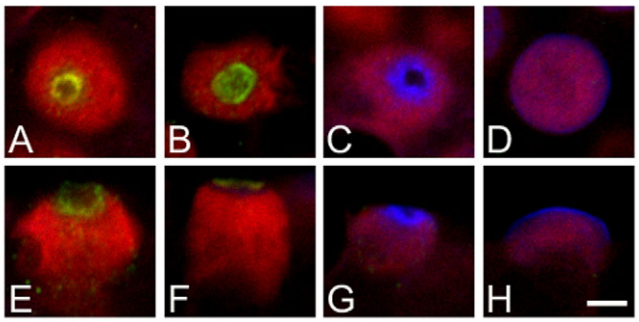

Fig. 5. Horizontal sections (A–D) and cross-sections (E–H) of mitochondria-rich (MR) cells, stained immunocytochemically with anti-Na^+/K^+-ATPase (red), anti-NHE3 (green) and anti-NCC (blue). (A,C,E,G) Gill MR cells with small pits immunoreactive to NHE3 (A,E) and NCC (C,G) in tilapia acclimated to normal Na^+/normal Cl^- water. (B,D,F,H) MR cells with enlarged apical membranes immunoreactive to NHE3 (B,F) and NCC (D,H) in tilapia acclimated to low Na^+/low Cl^- and normal Na^+/low Cl^- waters, respectively. Scale bar, 5 μm.

Considering that the function of apical NHE3 and NCC is to transport ions, mechanisms must exist to establish a favorable chemical gradient across the apical membrane. The enlarged area of the basolateral membrane that incorporates Na^+/K^+-ATPase contributes to a decrease in intracellular Na^+ concentration, which is favorable for Na^+ and Cl^- uptake through NHE3 and NCC. Moreover, it has been suggested that carbonic anhydrase may provide another driving force for NHE3 by producing H^+ and HCO_3^- (Evans et al., 2005). So far, some studies have demonstrated the

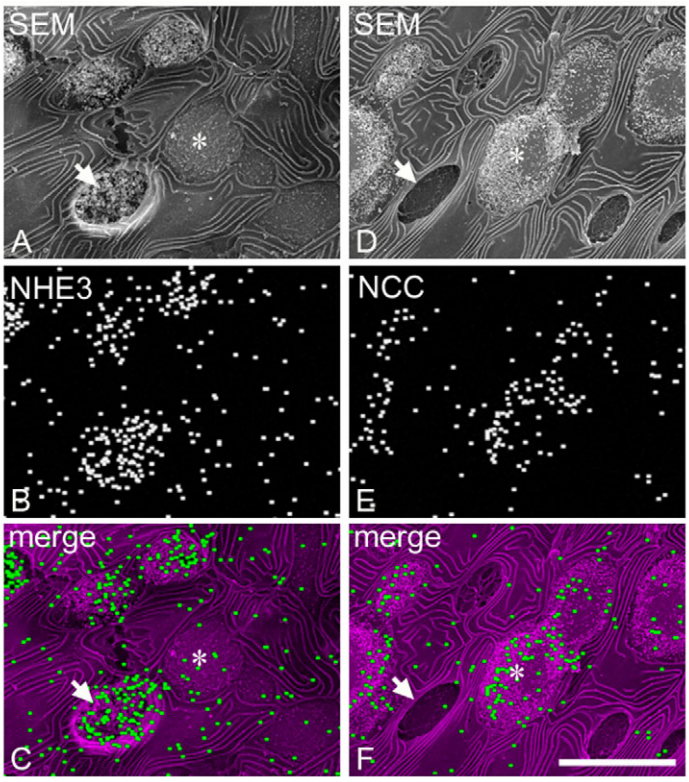

Fig. 6. Scanning electron microscopy immunocytochemistry for Na^+/H^+ exchanger-3 (NHE3) and Na^+/Cl^- cotransporter (NCC) in the gills of tilapia acclimated to artificial freshwaters with low Na^+/low Cl^- (A–C) and with normal Na^+/low Cl^- (D–F), respectively. (A,D) Scanning electron microscopic images. (B,E) X-ray signals specific for Ag indicating the presence of NHE3 (B) and NCC (E). (C,F) Merged images. NHE3 (B) and NCC (E) are confined to the concave (arrows) and convex (asterisks) apical surfaces, respectively. Scale bar, 10 μm.

existence of cytoplasmic carbonic anhydrase in gill MR cells and/or other ionocytes in rainbow trout (Rahim et al., 1988; Georgalis et al., 2006), flounder (Sender et al., 1999) and Osorezan dace (Hirata et al., 2003). In the zebrafish embryonic skin, both carbonic anhydrase 2-like a and carbonic anhydrase 15a mRNAs are localized in H^+-ATPase-rich cells, which contain NHE3b in their apical membrane (Esaki et al., 2007; Yan et al., 2007; Lin et al., 2008).

Our previous studies showed that the MR-cell population of tilapia acclimated to hypotonic water consisted mostly of MR cells with apical NHE3 and those with apical NCC, suggesting that these were ion-absorbing cells (Hiroi et al., 2008; Inokuchi et al., 2008). In the present study using whole-mount immunocytochemistry, both apical-NHE3 and apical-NCC cells were observed in all experimental groups, although the size of NHE3- and NCC-immunoreactive regions differed greatly depending on environmental Na^+ and Cl^- concentrations. NHE3-immunoreactive apical regions became larger in low Na^+ environments (the LowNa and LowNa/LowCl groups) than in normal Na^+ concentrations (Control and LowCl groups), and the enlarged apical regions appeared as concave or flat disks. Conversely, enlarged NCC-immunoreactive regions were convex in low Cl^- environments (LowCl and LowNa/LowCl groups). Those morphological characteristics of NHE3- and NCC-immunoreactive regions were consistent with SEM observations, suggesting that NHE3 and NCC are localized in concave and convex apical surfaces, respectively.

To further confirm the relationship between the localization of NHE3/NCC and the structure of apical surfaces, we compared the immunocytochemical images of NHE3/NCC distribution with the SEM images obtained simultaneously. For this purpose, we used the gills of tilapia acclimated to LowNa/LowCl and LowCl for detection of NHE3 and NCC, respectively, because the mRNA expression was higher in these respective groups. Using this technique, when the target ion transporter exists in the concave or convex apical surface of MR cells, the apical structure is lightly dusted with Ag precipitate, which impairs the visualization of the fine surface structures. In particular, the mesh-like structure of the concave apical surface is be indistinct, as compared with conventional SEM images. Nevertheless, X-ray signals indicating the presence of NHE3 were not detected in distinct convex apical surfaces but concentrated on concave apical surfaces dusted with Ag precipitate, indicating that NHE3 is confined to concave-apical MR cells. Conversely, X-ray signals for NCC were specific to convex apical surfaces. These findings provide direct evidence that NHE3 is located in the concave apical surface and NCC is in the convex apical surface.

In tilapia, different morphological and functional classifications of MR cells into subtypes have been adopted so far by different researchers. As described above, three subtypes of MR cells (wavy convex, shallow basin and deep hole) were proposed in freshwater tilapia, based on SEM observations (Lee et al., 1996). More recently, four subtypes (I–IV) of MR cells were identified according to different distribution patterns of Na^+/K^+-ATPase, $Na^+/K^+/2Cl^-$ cotransporter-1a (NKCC1a), cystic fibrosis transmembrane conductance regulator (CFTR) Cl^- channel, NCC and NHE3 in the tilapia embryonic skin (Hiroi et al., 2005; Hiroi et al., 2008). Among them, one type of ion-absorbing cells (type-II MR cells), in which NCC was localized in the apical membrane, was considered to be identical to wavy-convex MR cells (Hiroi et al., 2005; Hiroi et al., 2008). Our results using SEM immunocytochemistry confirm that apical-NCC cells were identical to convex-apical MR cells, or wavy-convex MR cells. Furthermore, we clearly show that apical-NHE3 MR cells, corresponding to type-III MR cells according to Hiroi et al. (Hiroi et al., 2008), possessed concave apical surfaces.

In the Control group, both NHE3 and NCC were detected in the apical regions of MR cells, although their immunoreactive apical regions were small and distinct from those typically observed in low Na^+ and Cl^- waters. Similarly, SEM observations showed that small apical pits of MR cells were more numerous than concave and convex apical surfaces in the Control fish. These findings suggest that NHE3 and NCC are also located in small apical pits. It is most likely that both apical-NHE3 cells and apical-NCC cells with small apical pits are less active or inactive when ambient Na^+ and Cl^- concentrations are similar to those in normal freshwater. With decreasing environmental Na^+ and Cl^- levels, however, apical-NHE3 cells and apical-NCC cells are activated and develop the large apical surfaces to facilitate ion absorption. In tilapia, most deep-hole MR cells (cells with a small apical pit in this study) were transformed into wavy-convex cells (cells with a convex apical surface) within 6 h, when tilapia were transferred from artificial high-Cl^- to low-Cl^- media (Chang et al., 2003). It is suggested that acute modification of MR-cell apical surface area is adjusted by the actin cytoskeleton at the apex of MR cells (Daborn et al., 2001; Chang et al., 2003). In addition to Cl^- concentration, the present study indicated that ambient Na^+ levels also affected the apical-surface morphology of MR cells. With increasing demand for deficient ions, small apical pits are considered to develop into concave apical surfaces in low Na^+ conditions, and into convex apical surfaces in low Cl^- conditions.

This is the first study to demonstrate directly the relationship between the apical membrane structures of MR cells observed by SEM and the apical localization of ion-transport proteins. As is the case with rainbow trout (Goss et al., 2001; Ivanis et al., 2008) and zebrafish (Pan et al., 2005; Lin et al., 2006; Hwang and Lee, 2007; Yan et al., 2007), it has been shown that ion-absorbing MR cells consist of functionally distinct cell types with different molecular mechanisms in tilapia. In addition, morphological studies have shown various apical structures of ion-absorbing MR cells. Our findings successfully integrated morphological and functional classifications of ion-absorbing MR cells in tilapia, although morpho-functional classifications may differ in different teleost species.

LIST OF ABBREVIATIONS

CFTR	cystic fibrosis transmembrane conductance regulator
Control	artificial freshwater with normal Na^+/normal Cl^-
LowCl	artificial freshwater with normal Na^+/low Cl^-
LowNa	artificial freshwater with low Na^+/normal Cl^-
LowNa/LowCl	artificial freshwater with low Na^+/low Cl^-
MR cell	mitochondria-rich cell
NCC	Na^+/Cl^- cotransporter
NHE3	Na^+/H^+ exchanger-3
NKCC1a	$Na^+/K^+/2Cl^-$ cotransporter-1a
SEM	scanning electron microscopy
V-ATPase	vacuolar-type H^+-ATPase

REFERENCES

Chang, I. C., Lee, T. H., Yang, C. H., Wei, Y. Y., Chou, F. I. and Hwang, P. P. (2001). Morphology and function of gill mitochondria-rich cells in fish acclimated to different environments. *Physiol. Biochem. Zool.* **74**, 111-119.

Chang, I. C., Lee, T. H., Wu, H. C. and Hwang, P. P. (2002). Effects of environmental Cl^- levels on Cl^- uptake and mitochondria-rich cell morphology in gills of the stenohaline goldfish, *Carassius auratus*. *Zool. Stud.* **41**, 236-243.

Chang, I. C., Wei, Y. Y., Chou, F. I. and Hwang, P. P. (2003). Stimulation of Cl^- uptake and morphological changes in gill mitochondria-rich cells in freshwater tilapia (*Oreochromis mossambicus*). *Physiol. Biochem. Zool.* **76**, 544-552.

Choe, K. P., Kato, A., Hirose, S., Plata, C., Sindic, A., Romero, M. F., Claiborne, J. B. and Evans, D. H. (2005). NHE3 in an ancestral vertebrate: primary sequence, distribution, localization, and function in gills. *Am. J. Physiol. Regul. Integr. Comp. Physiol.* **289**, R1520-R1534.

Daborn, K., Cozzi, R. R. F. and Marshall, W. S. (2001). Dynamics of pavement cell-chloride cell interactions during abrupt salinity change in *Fundulus heteroclitus*. *J. Exp. Biol.* **204**, 1889-1899.

Esaki, M., Hoshijima, K., Kobayashi, S., Fukuda, H., Kawakami, K. and Hirose, S. (2007). Visualization in zebrafish larvae of Na^+ uptake in mitochondria-rich cells whose differentiation is dependent on foxi3a. *Am. J. Physiol. Regul. Integr. Comp. Physiol.* **292**, R470-R480.

Evans, D. H., Piermarini, P. M. and Choe, K. P. (2005). The multifunctional fish gill: dominant site of gas exchange, osmoregulation, acid-base regulation, and excretion of nitrogenous waste. *Physiol. Rev.* **85**, 97-177.

Fenwick, J. C., Wendelaar Bonga, S. E. and Flik, G. (1999). *In vivo* bafilomycin-sensitive Na^+ uptake in young freshwater fish. *J. Exp. Biol.* **202**, 3659-3666.

Georgalis, T., Perry, S. F. and Gilmour, K. M. (2006). The role of branchial carbonic anhydrase in acid-base regulation in rainbow trout (*Oncorhynchus mykiss*). *J. Exp. Biol.* **209**, 518-530.

Goss, G. G., Perry, S. F. and Laurent, P. (1995). Ultrastructural and morphometric studies on ion and acid-base transport processes in freshwater fish. In *Fish physiology*, vol. 14 (ed. C. M. Wood and T. J. Shuttleworth), pp. 257-284. San Diego, CA: Academic Press.

Goss, G. G., Adamia, S. and Galvez, F. (2001). Peanut lectin binds to a subpopulation of mitochondria-rich cells in the rainbow trout gill epithelium. *Am. J. Physiol. Regul. Integr. Comp. Physiol.* **281**, R1718-R1725.

Hirata, T., Kaneko, T., Ono, T., Nakazato, T., Furukawa, N., Hasegawa, S., Wakabayashi, S., Shigekawa, M., Chang, M. H., Romero, M. F. et al. (2003). Mechanism of acid adaptation of a fish living in a pH 3.5 lake. *Am. J. Physiol. Regul. Integr. Comp. Physiol.* **284**, R1199-R1212.

Hiroi, J., McCormick, S. D., Ohtani-Kaneko, R. and Kaneko, T. (2005). Functional classification of mitochondrion-rich cells in euryhaline Mozambique tilapia (*Oreochromis mossambicus*) embryos, by means of triple immunofluorescence staining for Na^+/K^+-ATPase, $Na^+/K^+/2Cl^-$ cotransporter and CFTR anion channel. *J. Exp. Biol.* **208**, 2023-2036.

Hiroi, J., Yasumasu, S., McCormick, S. D., Hwang, P. P. and Kaneko, T. (2008). Evidence for an apical Na^+-Cl^- cotransporter involved in ion uptake in a teleost fish. *J. Exp. Biol.* **211**, 2584-2599.

Hirose, S., Kaneko, T., Naito, N. and Takei, Y. (2003). Molecular biology of major components of chloride cells. *Comp. Biochem. Physiol. B Biochem. Mol. Biol.* **136**, 593-620.

Hwang, P. P. and Lee, T. H. (2007). New insights into fish ion regulation and mitochondrion-rich cells. *Comp. Biochem. Physiol. A Mol. Integr. Physiol.* **148**, 479-497.

Inokuchi, M., Hiroi, J., Watanabe, S., Lee, K. M. and Kaneko, T. (2008). Gene expression and morphological localization of NHE3, NCC and NKCC1a in branchial mitochondria-rich cells of Mozambique tilapia (*Oreochromis mossambicus*) acclimated to a wide range of salinities. *Comp. Biochem. Physiol. A Mol. Integr. Physiol.* **151**, 151-158.

Ivanis, G., Esbaugh, A. J. and Perry, S. F. (2008). Branchial expression and localization of SLC9A2 and SLC9A3 sodium/hydrogen exchangers and their possible role in acid-base regulation in freshwater rainbow trout (*Oncorhynchus mykiss*). *J. Exp. Biol.* **211**, 2467-2477.

Kaneko, T., Watanabe, S. and Lee, K. M. (2008). Functional morphology of mitochondrion-rich cells in euryhaline and stenohaline teleosts. *Aqua Biosci. Monogr.* **1**, 1-62.

Katoh, F., Hyodo, S. and Kaneko, T. (2003). Vacuolar-type proton pump in the basolateral plasma membrane energizes ion uptake in branchial mitochondria-rich cells of killifish, *Fundulus heteroclitus*, adapted to a low ion environment. *J. Exp. Biol.* **206**, 793-803.

Laurent, P., Chevalier, C. and Wood, C. M. (2006). Appearance of cuboidal cells in relation to salinity in gills of *Fundulus heteroclitus*, a species exhibiting branchial Na^+ but not Cl^- uptake in freshwater. *Cell Tissue Res.* **325**, 481-492.

Lee, T. H., Hwang, P. P., Lin, H. C. and Huang, F. L. (1996). Mitochondria-rich cells in the branchial epithelium of the teleost, *Oreochromis mossambicus*, acclimated to various hypotonic environment. *Fish Physiol. Biochem.* **15**, 513-523.

Lee, T. H., Hwang, P. P., Shieh, Y. E. and Lin, C. H. (2000). The relationship between 'deep-hole' mitochondria-rich cells and salinity adaptation in the euryhaline teleosts, *Oreochromis mossambicus*. *Fish Physiol. Biochem.* **23**, 133-140.

Lin, L. Y. and Hwang, P. P. (2004). Mitochondria-rich cell activity in the yolk-sac membrane of tilapia (*Oreochromis mossambicus*) larvae acclimatized to different ambient chloride levels. *J. Exp. Biol.* **207**, 1335-1344.

Lin, L. Y., Horng, J. L., Kunkel, J. G. and Hwang, P. P. (2006). Proton pump-rich cell secretes acid in skin of zebrafish larvae. *Am. J. Physiol. Cell Physiol.* **290**, C371-C378.

Lin, T. Y., Liao, B. K., Horng, J. L., Yan, J. J., Hsiao, C. D. and Hwang, P. P. (2008). Carbonic anhydrase 2-like a and 15a are involved in acid-base regulation and Na uptake in zebrafish H-ATPase-rich cells. *Am. J. Physiol. Cell Physiol.* **294**, C1250-C1260.

Marshall, W. S. (2002). Na^+, Cl^-, Ca^{2+} and Zn^{2+} transport by fish gills: retrospective review and prospective synthesis. *J. Exp. Zool.* **293**, 264-283.

Marshall, W. S. and Grosell, M. (2006). Ion transport, osmoregulation and acid-base balance. In *The Physiology of Fishes* (ed. D. H. Evans and J. B. Claiborne), pp. 177-230. Boca Raton, FL: CRC Press.

Matey,V., Richards, J. G., Wang, Y., Wood, C. M., Rogers, J., Davies, R., Murray, B. W., Chen, X.-Q., Du, J. and Brauner, C. J. (2008). The effect of hypoxia on gill morphology and ionoregulatory status in the Lake Qinghai scaleless carp, *Gymnocypris przewalskii*. *J. Exp. Biol.* **211**, 1063-1074.

Pan, T. C., Liao, B. K., Huang, C. J., Lin, L. Y. and Hwang, P. P. (2005). Epithelial Ca^{2+} channel expression and Ca^{2+} uptake in developing zebrafish. *Am. J. Physiol. Regul. Integr. Comp. Physiol.* **289**, R1202-R1211.

Perry, S. F. (1997). The chloride cell: structure and function in the gills of freshwater fishes. *Annu. Rev. Physiol.* **59**, 325-347.

Perry, S. F., Goss, G. G. and Laurent, P. (1992). The interrelationships between gill chloride cell morphology and ionic uptake in four freshwater teleosts. *Can. J. Zool.* **70**, 1775-1786.

Perry, S. F., Shahsavarani, A., Georgalis, T., Bayaa, M., Furimsky, M. and Thomas, S. L. (2003). Channels, pumps, and exchangers in the gill and kidney of freshwater fishes: their role in ionic and acid-base regulation. *J. Exp. Zool.* **300**, 53-62.

Pisam, M., Caroff, A. and Rambourg, A. (1987). Two types of chloride cells in the gill epithelium of a freshwater-adapted euryhaline fish: *Lebistes reticulatus*; their modifications during adaptation to saltwater. *Am. J. Anat.* **179**, 40-50.

Pisam, M., Boeuf, G., Prunet, P. and Rambourg, A. (1990). Ultrastructural features of mitochondria-rich cells in stenohaline freshwater and seawater fishes. *Am. J. Anat.* **187**, 21-31.

Pisam, M., Le Moal, C., Auperin, B., Prunet, P. and Rambourg, A. (1995). Apical structures of "mitochondria-rich" alpha and beta cells in euryhaline fish gill: their behaviour in various living conditions. *Anat. Rec.* **241**, 13-24.

Rahim, S. M., Delaunoy, J. P. and Laurent, P. (1988). Identification and immunocytochemical localization of two different carbonic anhydrase isoenzymes in teleostean fish erythrocytes and gill epithelia. *Histochemistry* **89**, 451-459.

Sender, S., Böttcher, K., Cetin, Y. and Gros, G. (1999). Carbonic anhydrase in the gills of seawater- and freshwater-acclimated flounders *Platichthys flesus*: purification, characterization, and immunohistochemical localization. *J. Histochem. Cytochem.* **47**, 43-50.

Tang, C. H., Chang, I. C., Chen, C. H., Lee, T. H. and Hwang, P. P. (2008). Phenotypic changes in mitochondrion-rich cells and responses of Na^+/K^+-ATPase in gills of tilapia exposed to deionized water. *Zool. Sci.* **25**, 205-211.

Uchida, K., Kaneko, T., Miyazaki, H., Hasegawa, S. and Hirano, T. (2000). Excellent salinity tolerance of Mozambique tilapia (*Oreochromis mossambicus*): Elevated chloride cell activity in the branchial and opercular epithelia of the fish adapted to concentrated seawater. *Zool. Sci.* **17**, 149-160.

Watanabe, S., Inokuchi, M., Maruyama, T. and Kaneko, T. (2008). Na^+/H^+ exchanger isoform 3 expressed in apical membrane of gill mitochondrion-rich cells in Mozambique tilapia *Oreochromis mossambicus*. *Fish. Sci.* **74**, 813-821.

Wilson, J. M., Laurent, P., Tufts, B. L., Benos, D. J., Donowitz, M., Vogl, A. W. and Randall, D. J. (2000). NaCl uptake by the branchial epithelium in freshwater teleost fish: an immunological approach to ion-transport protein localization. *J. Exp. Biol.* **203**, 2279-2296.

Wilson, J. M., Whiteley, N. M. and Randall, D. J. (2002). Ionoregulatory changes in the gill epithelia of coho salmon during seawater acclimation. *Physiol. Biochem. Zool.* **75**, 237-249.

Yan, J. J., Chou, M. Y., Kaneko, T. and Hwang, P. P. (2007). Gene expression of Na^+/H^+ exchanger in zebrafish H^+-ATPase-rich cells during acclimation to low-Na^+ and acidic environments. *Am. J. Physiol. Cell. Physiol.* **293**, C1814-C1823.